Extracting the Condensate Density from Projection Experiments with Fermi Gases

A. Perali, P. Pieri, and G. C. Strinati
Dipartimento di Fisica, Università di Camerino, I-62032 Camerino, Italy
(Received 26 January 2005; published 30 June 2005)

A debated issue in the physics of the BCS-BEC crossover with trapped Fermi atoms is to identify characteristic properties of the superfluid phase. Recently, a condensate fraction was measured on the BCS side of the crossover by sweeping the system in a fast (nonadiabatic) way from the BCS to the Bose-Einstein condensation (BEC) sides, thus "projecting" the initial many-body state onto a molecular condensate. We analyze here the theoretical implications of these projection experiments, by identifying the appropriate quantum-mechanical operator associated with the measured quantities and relating them to the many-body correlations occurring in the BCS-BEC crossover. Calculations are presented over wide temperature and coupling ranges, by including pairing fluctuations on top of the mean field.

DOI: 10.1103/PhysRevLett.95.010407 PACS numbers: 03.75.Hh, 03.75.Ss

The current experimental advances with trapped Fermi atoms have attracted much interest in the physics of the BCS-BEC (Bose-Einstein condensate) crossover. In this context, one of the most debated issues is the unambiguous detection of superfluid properties on the BCS side of the crossover. Several attempts have been made in this direction. They include absorption images of the "projected" density profiles for ^{40}K [1] and ^{6}Li [2], rf spectroscopy to detect single-particle excitations [3], and measurements of collective modes [4,5]. In addition, a number of schemes to detect superfluid properties on the BCS side of the crossover have been proposed, including Josephson oscillations [6] and vortices [7].

In particular, the experimental procedure of Refs. [1,2] pairwise "projects" fermionic atoms onto molecules by preparing the system of trapped Fermi atoms on the BCS side with a tunable Fano-Feshbach resonance and then rapidly sweeping the magnetic field to the BEC side. In this way, the same two-component fit of density profiles routinely used for Bose gases is exploited to extract from these projected density profiles the analog of a condensate fraction, which is now associated with the equilibrium state on the BCS side before the sweep took place.

The purpose of this Letter is to provide a theoretical interpretation of the experiments of Refs. [1,2] by obtaining the projected density profiles in terms of the correlation functions of the Fermi gas at equilibrium. This is based on a number of physical assumptions that we associate with the experimental procedure of Refs. [1,2]. Our calculation evidences how the projection procedure amplifies the visibility of the emergence of the condensate as the temperature is lowered below the critical temperature T_c, when compared with the ordinary density profiles of Ref. [8]. We also attempt an analysis of the projected density profiles in terms of a two-component fit, in analogy to what is done with the experimental data [1,2]. A prediction is further made of a reduced molecular fraction that depends on the initial many-body state, in agreement with late experimental evidence [9].

The inclusion of pairing fluctuations on top of the mean field along the lines of Ref. [10] enables us to cover a wide temperature range even in the intermediate- and strong-coupling regimes, in contrast to Refs. [11,12] where only the mean field was taken into account.

To account for the projected density profiles of Refs. [1,2], we consider the bosonlike field operator:

$$\Psi_B(\mathbf{r}) = \int d\boldsymbol{\rho}\phi(\rho)\psi_\downarrow(\mathbf{r}-\boldsymbol{\rho}/2)\psi_\uparrow(\mathbf{r}+\boldsymbol{\rho}/2). \quad (1)$$

Here, $\psi_\sigma(\mathbf{r})$ is a fermion field operator with spin σ, and $\phi(\rho)$ is a real and normalized function that specifies the probability amplitude for the fermion pair. An operator of the form (1) was considered in Ref. [13] to obtain the condensate density for composite bosons.

Our theoretical analysis of the experiments of Refs. [1,2] is based on the following *physical assumptions* that we infer from the experimental procedure: (i) Atoms of a specific spin state were detected, which originate from the dissociation of molecules after applying an rf pulse. The object of the measurement is thus the bosonic (molecular) density $n_B(\mathbf{r})$ at position $\mathbf{r}$ [and not the fermionic (atomic) density $n(\mathbf{r})$]. (ii) A rather large conversion efficiency into molecules results when rapidly sweeping the magnetic field in the experiments. This suggests that molecules form just past the unitarity limit on the BEC side, where the "final" molecular wave function and the many-body correlations for the "initial" states considered in Refs. [1,2] have maximum overlap. Correspondingly, we assume that the wave function in the expression (1) refers to this final coupling, and represent it by $\phi_f(\rho)$. As molecules form in a medium, we take into account the effect of Pauli blocking in analogy with the original Cooper argument [14] and identify $\phi_f(\rho)$ with the bound-state solution of the two-body problem, with the condition that its Fourier transform $\phi_f(\mathbf{k})$ vanishes when the magnitude of the wave vector $\mathbf{k}$ is smaller than a characteristic value $k_{\mu_f} = \sqrt{2m\mu_f}$ for $\mu_f > 0$ (m being the fermion mass), while

no constraint is enforced for $\mu_f < 0$. Here, the value of the chemical potential μ_f depends on the final coupling at which the molecular state is assumed to form, thus implying that some sort of local equilibrium can be established around a molecule. We present our calculations for two final couplings that bound the interval where the maximum overlap occurs, and are at the same time representative of the two cases where μ_f is positive or negative. (iii) In the experiments, bosonic Thomas-Fermi (TF) profiles for the molecular condensate were extracted from position-dependent density profiles, thus entailing an assumption of thermal equilibrium. We assume that this thermal equilibrium corresponds to the state prepared *before* the rapid sweep of the magnetic field. The validity of this assumption is supported by a recent experimental study of the formation time of a fermion-pair condensate [9]. In our calculations, we then use $\langle \cdots \rangle_i$ as expressions for the thermal averages, where the suffix i stands for initial.

All these assumptions are summarized by stating that the *projected bosonic density profile* given by

$$n_B^{fi}(\mathbf{r}) = \langle \Psi_B^f(\mathbf{r})^\dagger \Psi_B^f(\mathbf{r}) \rangle_i \tag{2}$$

represents the *in situ* molecular density that would be measured after the rapid sweep but before the cloud expansion performed in Refs. [1,2] (the connection with the density measured after the expansion is discussed below). In this expression, the bosonlike field operator of Eq. (1) contains the *final* molecular wave function $\phi_f(\rho)$ on the BEC side of the crossover, while the thermal average $\langle \cdots \rangle_i$ is taken with reference to the state in which the system was *initially* prepared.

Consistently with our previous work [15], we describe the interaction term of the many-fermion Hamiltonian via an effective single-channel model. The parameter $(k_F a_F)^{-1}$ then drives the crossover from the BCS side [identified by $(k_F a_F)^{-1} \lesssim -1$] to the BEC side [identified by $1 \lesssim (k_F a_F)^{-1}$] across the unitarity limit $(k_F a_F)^{-1} = 0$. Here, a_F is the two-fermion scattering length, and the Fermi wave vector k_F results by setting $k_F^2/(2m)$ equal to the noninteracting Fermi energy.

The calculation proceeds by expressing the four-fermion field operator in Eq. (2) in terms of the two-particle Green's function $\mathcal{G}_2(1, 2, 1', 2') = \langle T_\tau[\Psi(1)\Psi(2)\Psi^\dagger(2')\Psi^\dagger(1')] \rangle$, where T_τ is the imaginary-time ordering operator. We have introduced the spinor $\Psi(\mathbf{r}) = (\psi_\uparrow(\mathbf{r}), \psi_\downarrow^\dagger(\mathbf{r}))$ as well as the shorthand notation $1 = (\mathbf{r}_1, \tau_1, \ell_1)$ with imaginary time τ and spinor component ℓ, such that $\Psi(1) = \exp\{K\tau_1\}\Psi_{\ell_1}(\mathbf{r}_1)\exp\{-K\tau_1\}$. The thermal average contains the grand-canonical Hamiltonian $K = H - \mu N$ with fermionic chemical potential μ and is taken in the initial state, as specified above.

The two-particle Green's function $\mathcal{G}_2$ is, in turn, expressed in terms of the many-particle T matrix by solving formally the Bethe-Salpeter equation as follows:

$$\mathcal{G}_2(1, 2, 1', 2') = \mathcal{G}(1, 1')\mathcal{G}(2, 2') - \mathcal{G}(1, 2')\mathcal{G}(2, 1') - \int d3456\, \mathcal{G}(1, 3)\mathcal{G}(6, 1')T(3, 5; 6, 4)\mathcal{G}(4, 2')\mathcal{G}(2, 5), \tag{3}$$

where $\mathcal{G}(1, 1') = -\langle T_\tau[\Psi(1)\Psi^\dagger(1')] \rangle$ is the fermionic single-particle Green's function. Accordingly, the projected bosonic density (2) reads

$$n_B^{fi}(\mathbf{r}) = \int d\boldsymbol{\rho} d\boldsymbol{\rho}' \phi_f(\rho)\phi_f(\rho')\mathcal{G}_2^i(1, 2, 1', 2'), \tag{4}$$

where $1 = (\mathbf{r} - \boldsymbol{\rho}/2, \tau + 2\eta, \ell = 2)$, $2 = (\mathbf{r} + \boldsymbol{\rho}'/2, \tau, \ell = 1)$, $1' = (\mathbf{r} + \boldsymbol{\rho}/2, \tau + 3\eta, \ell = 1)$, and $2' = (\mathbf{r} - \boldsymbol{\rho}'/2, \tau + \eta, \ell = 2)$ (η being a positive infinitesimal).

Implementation of the above expressions to the trapped case is readily obtained via a local-density approximation, whereby a local gap parameter $\Delta(\mathbf{r})$ is introduced and the chemical potential μ is replaced (whenever it occurs for both initial and final couplings) by the quantity $\mu(\mathbf{r}) = \mu - V(\mathbf{r})$ that accounts for the trapping potential $V(\mathbf{r})$.

The three terms on the right-hand side of Eq. (3) correspond to physically different contributions to expression (4). In particular, the first term can be written as $|\alpha_{fi}|^2$, where $\alpha_{fi} = \int d\boldsymbol{\rho}\phi_f(\rho)\mathcal{G}_{12}^{(i)}(\rho, \tau = -\eta)$ represents the *overlap* between the fermionic correlations (embodied in the anomalous single-particle Green's function $\mathcal{G}_{12}^{(i)}$) and the molecular wave function ϕ_f. This contribution vanishes with the gap parameter Δ when approaching T_c, and is identified with the *condensate density* for composite bosons when both the initial thermal equilibrium and the final molecular wave function are taken at the same coupling deep in the BEC region [13]. Only this contribution was considered in Ref. [12] in connection with the experiments of Refs. [1,2].

The second term on the right-hand side of Eq. (3) represents fermionic correlations in the normal state that are relevant in the presence of an underlying Fermi surface. This term is most sensitive to the final molecular wave function ϕ_f being affected by Pauli blocking when μ_f is positive. This term would be irrelevant if the initial thermal equilibrium and the final molecular wave function were taken deep in the BEC side. When μ_f is positive, this term can lead to an overestimate of the value of the condensate fraction when the projected density profiles are fitted in terms of TF and Gaussian functions, as argued below. Both this and the previous contribution were considered in Ref. [11] (where the final coupling was, however, taken deep in the BEC region).

The third term on the right-hand side of Eq. (3) is calculated in the following within the off-diagonal BCS-RPA approximation considered in Ref. [13]. This contri-

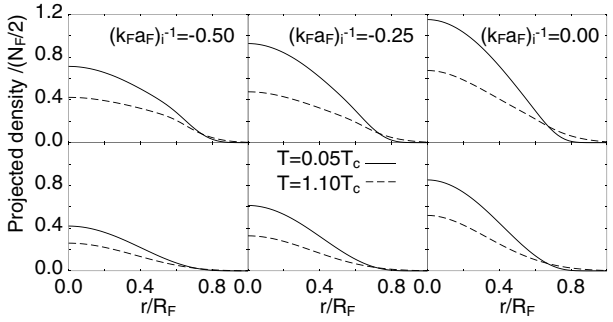

FIG. 1. Axially integrated projected density profiles (in units of R_F^{-2} where R_F is the fermionic Thomas-Fermi radius) for three initial coupling values and for two final couplings: 0.40 (upper panel) and 1.50 (lower panel).

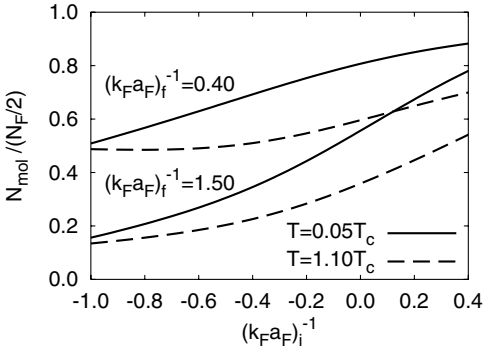

FIG. 2. Ratio $N_{\mathrm{mol}}/(N_F/2)$ vs $(k_F a_F)_i^{-1}$ for two temperatures and final couplings.

bution is identified with the *noncondensate density* for composite bosons when both the initial thermal equilibrium and the final molecular wave function are taken at the same coupling deep in the BEC side [13]. It is thus of particular importance for increasing temperature when approaching the normal phase.

When $i = f$ deep in the BEC region, the projected density profile $n_B^{ii}(\mathbf{r})$ coincides with (half) the ordinary density profile $n(\mathbf{r})$ calculated at the same coupling. In the following, the values for the local chemical potential and gap parameter, to be inserted in expression (4) for $n_B^{fi}(\mathbf{r})$, are obtained with the theory of Ref. [8] where pairing fluctuations are included on top of the mean field.

Figure 1 shows the axially integrated projected density profiles calculated for the coupling values $(k_F a_F)_i^{-1} = (-0.50, -0.25, 0.00)$ and for the two representative values 0.40 (upper panel) and 1.50 (lower panel) of the final coupling $(k_F a_F)_f^{-1}$. Two characteristic temperatures (just above the critical temperature and near zero temperature) are considered in each case. Note the marked temperature dependence of the projected density profiles when entering the superfluid phase, as signaled by the emergence of a ''condensate'' component near the center of the trap. This contrasts the milder dependence (especially on the BCS side) of the density profiles without projection [8]. The ''projection'' technique introduced in Ref. [1] is thus demonstrated to *amplify* the effects due to the presence of a condensate on the density profiles, which would otherwise be almost temperature independent on the BCS side of the crossover.

In Fig. 1 the densities are normalized to half the total number N_F of fermionic atoms. This number differs, in general, from the total number N_{mol} of molecules obtained by integrating the projected density profiles. In particular, N_{mol} can vary significantly when scanning the initial coupling $(k_F a_F)_i^{-1}$ on the BCS side of the crossover for the given final molecularlike state. This effect is shown in Fig. 2 for the same temperatures and final couplings of Fig. 1. Our finding that the total number N_{mol} of molecules constitutes only a fraction of the original atom number $N_F/2$ for each spin state is supported by the experimental results of Refs. [1,2]. In addition, our prediction that the reduced value of the molecular fraction depends on the initial many-body state is in agreement with the experimental evidence recently reported in Ref. [9]. Note that, for both values of the ''final coupling,'' the total number of molecules increases upon lowering the temperature. This result indicates that the conversion efficiency for the condensate fraction is larger than for the thermal component, as also observed in Ref. [9].

In our procedure, the *condensate* and *noncondensate* components of the projected density profiles are calculated separately. By our definition, they correspond to the first term and to the remaining terms on the right-hand side of Eq. (3), respectively. The *condensate fraction* is obtained accordingly from the ratio of the corresponding areas. Yet, the total projected density profiles obtained theoretically could be analyzed in terms of a two-component fit with a TF plus a Gaussian function (or, better, a $g_{3/2}$ function for the Bose gas), in analogy to a standard experimental procedure. This kind of analysis is reported in Fig. 3 for the two low-temperature curves shown in the right panels of Fig. 1. In both cases, a good overall fit is obtained by the χ-square method. A separate comparison is also made in the figure with the theoretical condensate and nonconden-

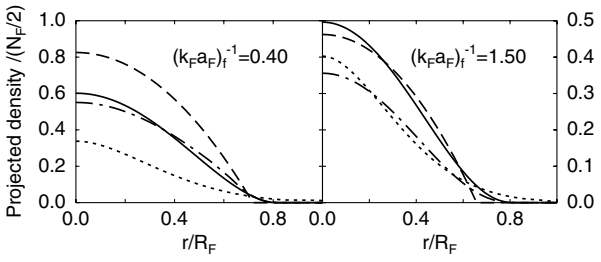

FIG. 3. Two-component (TF plus $g_{3/2}$) fit of the axially integrated projected density profiles (in units of R_F^{-2}) at the unitarity limit for $T/T_c = 0.05$. The TF (dashed line) and $g_{3/2}$ (dotted line) components of the fit are compared with the theoretical condensate (full line) and noncondensate (dash-dotted line) components.

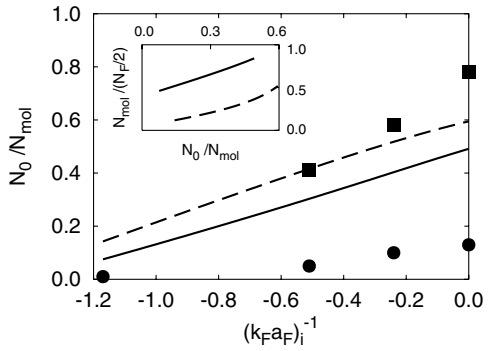

FIG. 4. Condensate fraction N_0/N_{mol} vs $(k_F a_F)_i^{-1}$ on the BCS side of the crossover at $T/T_c = 0.05$ and for the two final couplings 0.40 (full line) and 1.50 (dashed line). The data from the experiments of Refs. [1] (dots) and [2] (squares) are also reported. The inset shows $N_{\mathrm{mol}}/(N_F/2)$ vs N_0/N_{mol} for the same temperature and final couplings.

sate components defined above, which appears rather good for the value 1.50 of the final coupling, while for the value 0.40 an overestimate (of about 50%) of the condensate results from the fit. This discrepancy stems mostly from the second term on the right-hand side of Eq. (3), which contributes to the TF component of the fit owing to a peculiar shape of the corresponding projected density profile.

The extension of this analysis to initial couplings on the BCS side reveals unconventional forms of the theoretical condensed and noncondensed contributions to the projected density profiles, so that the above two-component fit fails. For negative values of the initial coupling when the two-component fit fails, we have verified that the difference $N_{\mathrm{mol}}(T=0) - N_{\mathrm{mol}}(T=1.10T_c)$ approximately coincides with $N_0(T=0)$ within a relative error not larger than 10% when $(k_F a_F)_f^{-1} = 0.4$. This suggests a practical prescription to extract $N_0(T=0)$ from the values of N_{mol} at low temperature and slightly above the critical temperature, without relying on a two-component fit.

In this respect, recall that our theoretical projected density profiles are calculated when molecules just form on the BEC side near the unitarity limit. In the experiments, however, a further ramp of the magnetic field is performed together with a subsequent cloud expansion. Only at this stage is the profile of the cloud detected. The comparison between theory and experiments is thus meaningful since the further ramp of the magnetic field and the subsequent cloud expansion are expected to have no influence on the values of N_{mol} and N_0/N_{mol}. This is because, by the further ramp, the molecules shrink adiabatically following the field. They then become tightly bound and weakly interacting among themselves, while their local counting is unaffected. Under these conditions, the condensate fraction, too, should not be modified by the subsequent expansion as it is the case for an ordinary dilute Bose gas, even though the expansion may affect the details of the density profiles.

In Fig. 4 the condensate fraction N_0/N_{mol}, obtained from our theoretical expressions at the lowest temperature $T/T_c = 0.05$, is plotted vs $(k_F a_F)_i^{-1}$ on the BCS side of the crossover. The data from Refs. [1,2] are also reported in the figure. The agreement between the overall trends of the theoretical and experimental curves appears satisfactory, although quantitative discrepancies result between the two sets of curves. They might be due to an overestimate of the TF component of the fits in Ref. [2] for the reasons discussed in Ref. [9], and to a possible underestimate of the condensate component in Ref. [1] due to a preferential loss of molecules in the condensate itself. We have, finally, verified that a linear dependence occurs between $N_{\mathrm{mol}}/(N_F/2)$ and N_0/N_{mol} (inset of Fig. 4). A similar linear dependence is also reported in Fig. 4(b) of Ref. [2], although with a different definition of N_{mol} that includes also molecular states not directly detected in the experiment.

We are indebted to C. Salomon and H. Stoof for discussions and to D. Jin for a critical reading of the manuscript. This work was partially supported by the Italian MIUR with Contract Cofin-2003 "Complex Systems and Many-Body Problems."

[1] C. A. Regal, M. Greiner, and D. S. Jin, Phys. Rev. Lett. **92**, 040403 (2004).
[2] M. W. Zwierlein *et al.*, Phys. Rev. Lett. **92**, 120403 (2004).
[3] C. Chin *et al.*, Science **305**, 1128 (2004).
[4] J. Kinast, S. L. Hemmer, M. E. Gehm, A. Turlapov, and J. E. Thomas, Phys. Rev. Lett. **92**, 150402 (2004).
[5] M. Bartenstein *et al.*, Phys. Rev. Lett. **92**, 203201 (2004).
[6] F. S. Cataliotti *et al.*, Science **293**, 843 (2001); G. Orso, L. P. Pitaevskii, and S. Stringari, Phys. Rev. Lett. **93**, 020404 (2004); M. Wouters, J. Tempere, and J. T. Devreese, Phys. Rev. A **70**, 013616 (2004).
[7] M. Greiner, C. A. Regal, and D. S. Jin, cond-mat/0502539.
[8] A. Perali, P. Pieri, L. Pisani, and G. C. Strinati, Phys. Rev. Lett. **92**, 220404 (2004).
[9] M. W. Zwierlein *et al.*, cond-mat/0412675.
[10] P. Pieri, L. Pisani, and G. C. Strinati, Phys. Rev. B **70**, 094508 (2004).
[11] R. B. Diener and T. L. Ho, cond-mat/0404517.
[12] A. V. Avdeenkov and J. L. Bohn, Phys. Rev. A **71**, 023609 (2005).
[13] N. Andrenacci, P. Pieri, and G. C. Strinati, Phys. Rev. B **68**, 144507 (2003).
[14] L. N. Cooper, Phys. Rev. **104**, 1189 (1956).
[15] S. Simonucci, P. Pieri, and G. C. Strinati, Europhys. Lett. **69**, 713 (2005).